Skeletal Radiol (2011) 40:439–446
DOI 10.1007/s00256-010-1018-x

SCIENTIFIC ARTICLE

Magnetic resonance imaging of intramuscular metastases

Alexey Surov · Eckhard Fiedler · Wieland Voigt · Andreas Wienke · Hans-Jürgen Holzhausen · Rolf-Peter Spielmann · Curd Behrmann

Received: 8 June 2010 / Revised: 27 July 2010 / Accepted: 28 July 2010 / Published online: 10 August 2010

Abstract
Objective The aim of the present study was to analyse magnetic resonance findings of intramuscular metastases (IM) in a relatively large series.
Materials and Methods From January 2000 to January 2010, 28 patients (207 metastases) were retrospectively identified in the radiological database of the Martin-Luther-University. Several different scanning protocols were used depending on the localisation of IM. In 12 patients diffusion-weighted (DW) images were obtained with a multi-shot SE-EPI sequence. Apparent diffusion coefficient (ADC) maps were also calculated. Furthermore, fusion images were manually generated between the DW and half-Fourier acquisition single-shot turbo spin echo (HASTE) images.
Results On T2-weighted images, 97% of the recognised IM were hyperintense in comparison to unaffected musculature, and 3% were mixed iso- to hyperintense. On T1-weighted images most IM (91%) were homogeneously isointense in comparison to muscle tissue, whereas 4% were hypointense, and 5% lightly hyperintense. ADC maps were calculated for 91 metastases ranging from 0.99 to 4.00 mm^2s^{-1} (mean value 1.99±0.66). ADC values of low (<1.5) signal intensity (SI) were identified in 26%, moderate SI (from 1.5 to 3.0) in 68%, and high SI (>3.0) in 6%. Of the IM that were investigated with contrast medium, 88.5% showed marked enhancement. It was homogeneous in 88% and heterogenous in 6%. Rim enhancement with central low attenuation was seen in 6%. There was no difference in enhancement characteristics with respect to ADC values or fusion patterns. Peritumoral enhancement was identified in 2.4%.
Conclusion Magnetic resonance features of muscle metastases are relatively typical and consist of round or oval intramuscular masses with well-defined margins, marked enhancement, low or moderate ADC values, and moderate to high signal intensity on fusion images.

Keywords Intramuscular metastases · MR imaging

A. Surov (✉) · R.-P. Spielmann · C. Behrmann
Department of Radiology,
Martin-Luther-University Halle-Wittenberg,
Halle, Germany
e-mail: alex.surow@medizin.uni-halle.de

E. Fiedler
Department of Dermatology and Venereology,
Martin-Luther-University Halle-Wittenberg,
Halle, Germany

W. Voigt
Department of Oncology,
Martin-Luther-University Halle-Wittenberg,
Halle, Germany

A. Wienke
Department of Biometry,
Martin-Luther-University Halle-Wittenberg,
Halle, Germany

H.-J. Holzhausen
Department of Pathology,
Martin-Luther-University Halle-Wittenberg,
Halle, Germany

Introduction

Skeletal muscles are refractory to metastatic disease [1–3]. They produce several anti-cancer factors, such as leukaemia inhibitory factor or interleukin-6, which inhibit proliferation of tumour cells [1]. Variable blood flow in skeletal muscles also plays a role [3]. Furthermore, cancer cells can be biomechanically damaged in the microvasculature of skeletal muscles [2]. Therefore, metastases in skeletal

musculature are rare [3–8]. As reported previously, the prevalence of intramuscular metastases (IM) varies in autopsy series from 0.03% to 5.6% [4–6] and in radiological series from 1.2% to 1.8% [7, 8].

Previously, computer tomographic patterns of muscle metastases have been described in a large series [8]. Although magnetic resonance (MR) imaging is the technique of choice for characterising soft tissue tumours, MR findings of IM have been reported only sporadically in the literature [7, 9–13]. Therefore, the aim of the present study was to analyse MR findings of IM in a relatively large series.

Materials and methods

This retrospective study was approved by the Institutional Ethics Committee.

The radiological database of the tertiary care centre was screened retrospectively in the time period from January 2000 to January 2010 for muscle involvement in oncological diseases (search for key words in the reports). Cases with direct invasion of the tumour into the skeletal musculature, patients with primary muscle sarcoma and primary or secondary muscle lymphoma were excluded from the study. Furthermore, only patients with muscle metastases investigated by MRI were included in the study. They were identified in 28 cases. There were 15 women and 13 men with a median age of 65 years, ranging from 41 to 79 years (Table 1).

Magnetic resonance imaging was performed using a 1.5-T MRI scanner (Magnetom Vision Sonata Upgrade; Siemens, Germany). Several different scanning protocols were used depending on lesion localisation. MRI sequences included T2-weighted (T2W) turbo spin echo images, fat-suppressed T2W short tau inversion recovery (STIR) images, half-Fourier acquisition single-shot turbo spin echo (HASTE) images, T1-weighted (T1W) spin echo (T1W SE) images, T1W flash 2D (FL 2D) images. Additionally, in 12 patients diffusion-weighted (DW) images were obtained with a multi-shot SE-EPI sequence. DW imaging parameters varied depending on the regions investigated (Table 2) and include generally b values of 0 and 600 s/mm^2; section thickness, 6 mm with no gap; and motion-probing gradient pulses placed in the three

Table 1 Patients, primary tumours and number of the identified intramuscular metastases (*IM*)

Patient number	Sex	Age	Diagnosis	Number of IM
1	Female	59	Pulmonary angiosarcoma	1
2	Female	65	Histiocytoma	2
3	Male	70	Melanoma	1
4	Female	45	Breast cancer	1
5	Female	50	Sarcoma	2
6	Male	59	Renal cell carcinoma	1
7	Female	71	Melanoma	1
8	Female	47	CUP	1
9	Female	68	Leiomyosarcoma of the uterus	2
10	Female	78	Carcinoma of the cervix	1
11	Female	68	Ovarian carcinoma	2
12	Male	67	Hepatocellular carcinoma	1
13	Male	64	Pancreas carcinoma	Multiple
14	Male	79	Melanoma	1
15	Male	65	Renal cell carcinoma	Multiple
16	Female	44	Thyroid gland carcinoma	1
17	Male	60	Oesophageal cancer	3
18	Male	67	Renal cell carcinoma	1
19	Male	72	Renal cell carcinoma	8
20	Female	41	Rectal cancer	2
21	Female	77	Bronchial carcinoma	2
22	Male	51	Melanoma	Multiple
23	Male	70	Renal cell carcinoma	1
24	Female	55	Leiomyosarcoma	2
25	Female	65	Breast cancer	2
26	Male	68	Renal cell carcinoma	1
27	Male	69	Gastric cancer	1
28	Female	65	Breast cancer	1

Table 2 Magnetic resonance features of intramuscular metastases

Features	Percentage
Form	
Round	80
Oval	14.5
Lobulated	5
Muscle infiltration	0.5
Margins	
Well-defined	96
Ill-defined	4
Signal intensity	
T1-weighted image	
Hyperintense	5
Isointense	91
Hypointense	4
T2-weighted image	
Mixed iso- to hyperintense	3
Hypointense	97
Apparent diffusion coefficient values	
Low	26
Moderate	68
High	6
Contrast enhancement	
Homogeneous	88
Heterogeneous	6
Rim enhancement	6
Fusion pattern	
No abnormal signal	47
Subtle signal increase	27
Moderate signal increase	20
Marked signal increase	6

orthogonal planes. Isotropic DW imaging was generated by three orthogonal axis images. Thus, apparent diffusion coefficient (ADC) maps were calculated on the operating console on a voxel-by-voxel basis with an algorithm implemented according to the following equation [14]:

$$\mathrm{ADC}\left(\mathrm{mm^2 s^{-1}}\right) = \left[\mathrm{In}\left(\mathrm{S^0}/\mathrm{S^{600}}\right]/600,$$

where S^0 and S^{600} represent the signal intensities of the images. The section with the largest diameter of the investigated metastasis was selected for ADC calculation. In that image a circular region of interest (ROI) as large as possible was selected without risking partial volume effects. Small metastases below 5 mm in diameter were excluded from the measurement. ADC values were classified as follows: low signal intensity<1.5, moderate signal intensity>1.5<3.0, and high signal intensity>3.0.

In addition, in 12 patients in whom DW imaging was performed, fusion images were manually generated between the DW (b values, 600 s/mm^2) and HASTE images using a workstation (Siemens Leonardo VD 10 B Syngo VX49B). The presence of abnormal signal on fusion images was graded as follows: 0=no abnormal signal, 1=subtle, but definitely increased signal, 2 = moderate signal intensity, 3 = marked signal intensity.

In 24 patients (201 lesions) T1W SE, T1W SE FS and/or T1 flash 2D images were repeated after intravenous administration of contrast medium (gadopentate dimeglumine; Magnevist, Bayer Schering Pharma, Leverkusen, Germany), 0.1 ml per kilogram of body weight.

Magnetic resonance images and secondary calculations of all patients were re-interpreted by two radiologists (A.S. and C.B., with 7 and 20 years of experience respectively). Consensus of the investigators was obtained on the following features of the metastases: number, shape, localisation, size, margin, attenuation, homogeneity and contrast enhancement.

The diagnosis of IM was confirmed histopathologically by muscle biopsy in 7 cases. In 9 cases soft tissue lesions of another localisation had been investigated pathologically. In 12 patients the diagnosis of IM was made on the basis of disease sequelae.

Collected data were evaluated by means of descriptive statistics (absolute and relative frequencies). ADC values in the different fusion groups were compared by means of a linear mixed model.

Results

The number of IM per patient ranged from 1 to 137 (Table 1). The following muscles were involved: gluteus maximus (24%), biceps femoris (19.3%), erector spinae (17.9%), quadriceps femoris (15.4%), iliopsoas (6.3%), adductor magnus (5.8%), gluteus medius (2.5%), latissimus dorsi (2.4%), trapezius (2%), quadratus lumborum (1.4%), tibialis anterior (1%), pectoralis (0.5%), brachialis (0.5%), teres major (0.5%), and deltoideus (0.5%). In most patients (n=24, 86%) IM were diagnosed incidentally during routine staging CT examinations. In 4 patients (14%) IM presented as painful masses. In all cases intramuscular masses were identified. They were round or oval in shape with a median size of 6 mm (range 2–125 mm).

Radiological findings are summarized in Table 2. On T2W images 97% of the recognized IM were hyperintense in comparison to unaffected musculature, and 3% were mixed iso- to hyperintense. On T1W images most of the IM (91%) were homogeneously isointense compared with muscle tissue, whereas 4% were hypointense, and 5% lightly hyperintense. On T2W images with fat saturation surrounding oedema was seen in 1.5%.

Apparent diffusion coefficient (ADC) maps were calculated for 91 metastases ranging from 0.99 to 4.00 mm^2s^{-1} (mean value 1.99±0.66). Low ADC values (< 1.5) were identified in 26%, moderate ADC values (from 1.5 to 3.0) in 68%, and high ADC values (> 3.0) in 6%.

On fusion between DWI and HASTE images most lesions (47%) showed no abnormal signal. In 27% a subtle signal increase was seen (Fig. 1), in 20% the signal increase was moderate (Fig. 2), and in 6% high (Fig. 3).

Apparent diffusion coefficient values dependent on signal increase on fusion images are shown in Table 3. Figure 3 shows that the higher the signal was on fusion images, the lower were the corresponding ADC values. The ADC values were significantly higher in the fusion group without abnormal signal than in the group with light signal abnormalities (2.4 vs 1.8, p=0.001). Furthermore, the ADC values were significantly higher in the fusion group with a subtle signal increase than in the moderate signal increase group (1.8 vs 1.4, p=0.001). Thus, there was no significant difference in ADC values between the fusion groups with moderate and high signal increase (1.4 vs 1.2, p=0.175).

After intravenous administration of contrast medium most lesions (88.5%) showed a marked enhancement. It was homogeneous in 88% and heterogeneous in 6%. Rim enhancement with central low attenuation was seen in 6%. There was no difference in enhancement characteristics with respect to ADC values or fusion patterns. Therefore, considerably more IM were seen after contrast administration

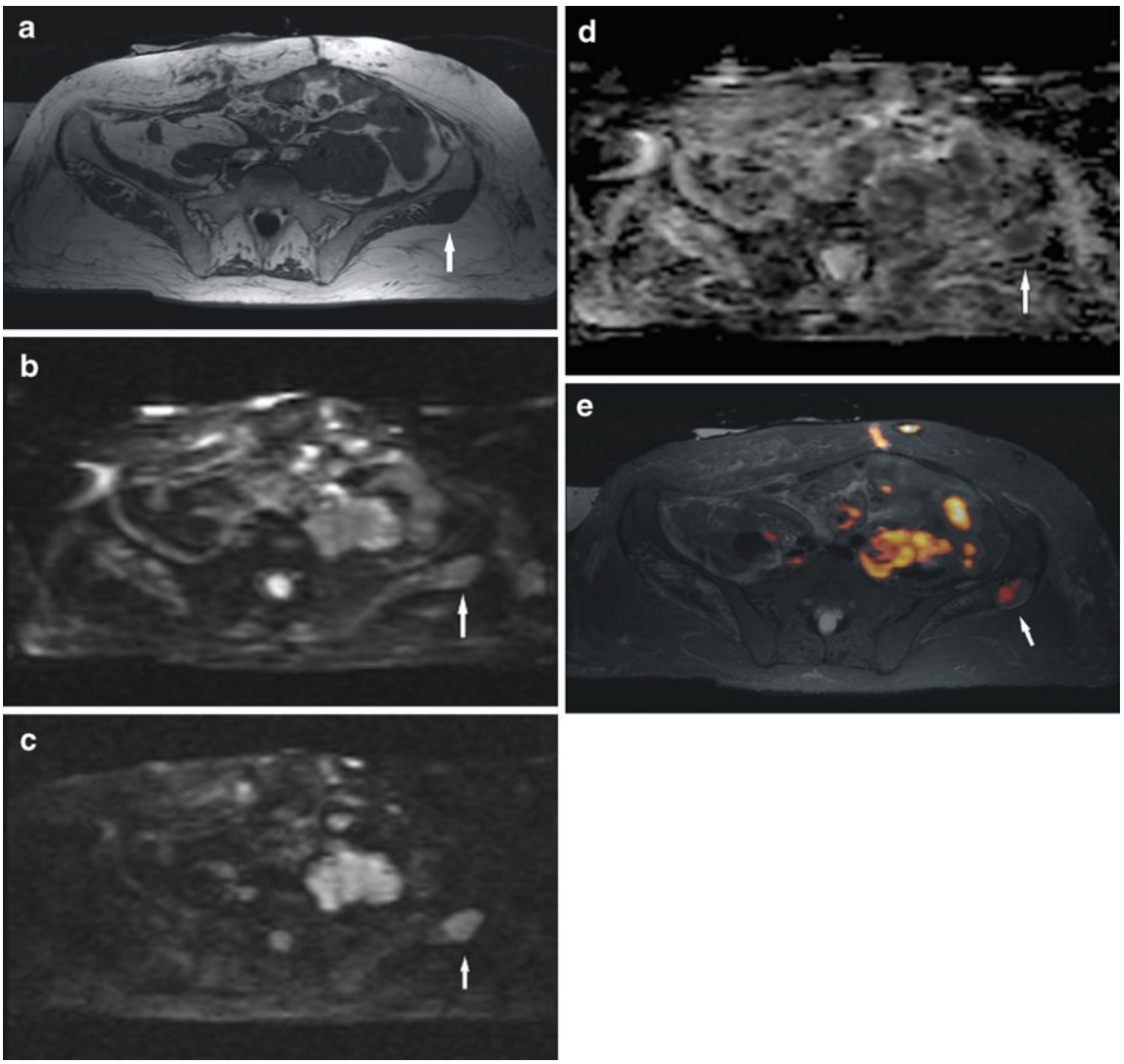

Fig. 1 Intramuscular metastasis (*arrow*) in the left gluteal musculature in a patient with ovarian cancer. **a** On T1-weighted (T1W) images (SE, TR/TE: 569/11) the lesion shows similar signal to muscles (*arrow*). **b** Diffusion-weighted image (DWI; TR/TE: 5,000/68) of the metastasis with a b-value of 0 s/mm^2. **c** DWI (TR/TE: 5,000/68) of the metastasis with a b-value of 600 s/mm^2. **d** Corresponding apparent diffusion coefficient (ADC) map of DWI indicating moderate cellularity (1.55×10^{-3} mm^2s^{-1}). **e** Fusion image between DWI and half-Fourier acquisition single-shot turbo spin echo (HASTE) images shows a light signal increase within the metastasis (*arrow*). Additionally, marked signal increase of the peritoneal tissue is seen (known peritoneal carcinosis)

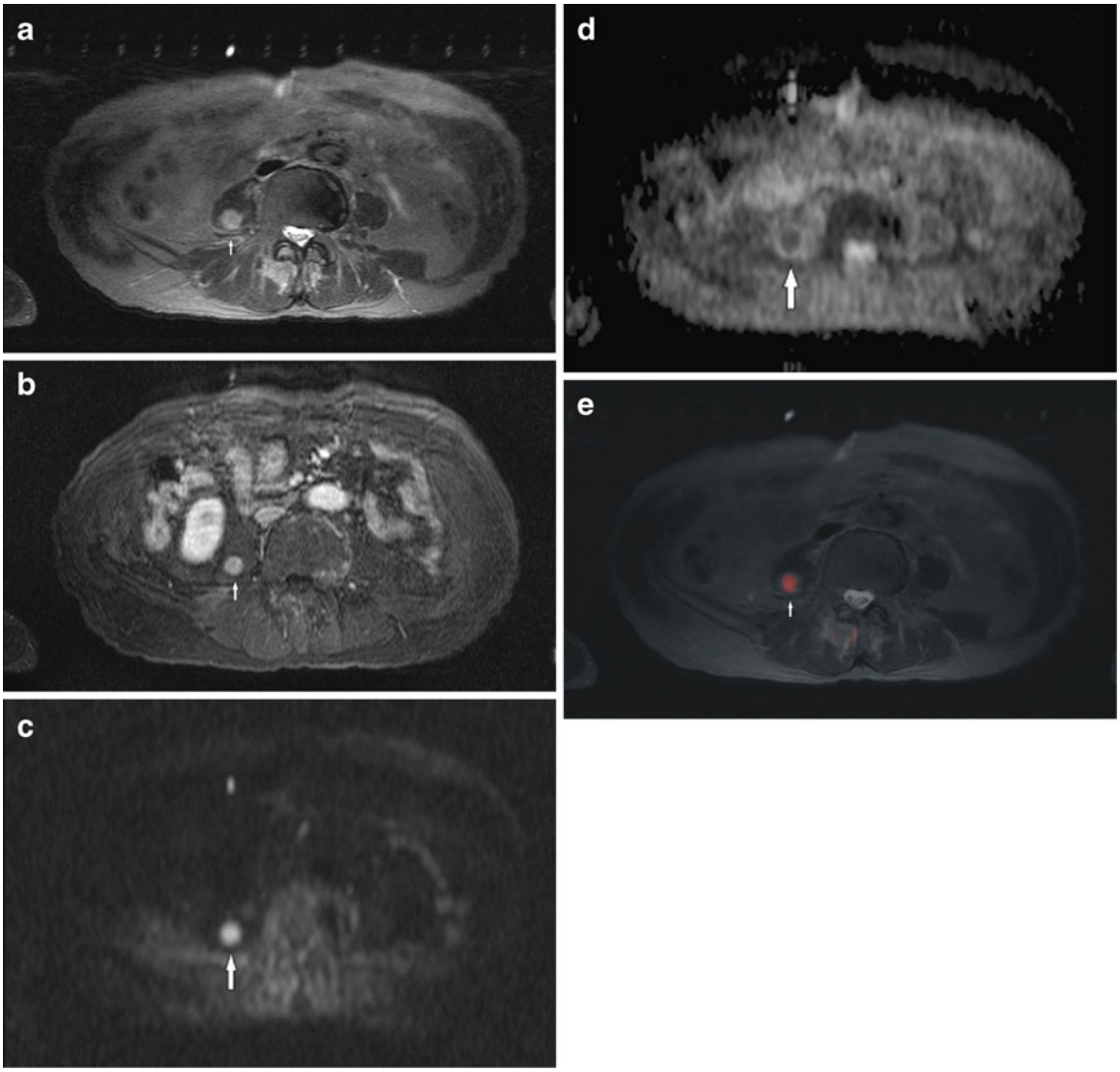

Fig. 2 Intramuscular metastasis in the right iliopsoas muscle (*arrow*) in a patient with gastric cancer. **a** On HASTE images (TR/TE: 806/105) the metastasis is hyperintense in comparison to the normal musculature. **b** T1W image with fat saturation after administration of contrast medium (SE, TR/TE: 762/12) shows the high signal intensity of the lesion. There is no surrounding oedema. **c** DWI (TR/TE: 5000/68) of the metastasis with a b-value of 600 s/mm^2. **d** Corresponding ADC map of DWI indicating high cellularity (1.20×10^{-3} mm^{2}s^{-1}). **e** Fusion image between DWI and HASTE images shows a moderate signal increase within the metastasis (*arrow*)

than on fusion images (Fig. 3). Peritumoral enhancement was identified in 2.4%.

Discussion

The previously reported MRI appearances of muscle metastases have been inconsistent [9–13]. Only a few radiological studies with small series examined IM on MRI [9, 10, 13]. For example, Glockner et al. analysed 5 cases of IM [7]. In their study the IM identified were investigated without intravenous application of contrast medium, thereby restricting the interpretation of the images. Furthermore, in the series of Lee et al. only 8 IM were identified [13]. Other publications regarding MR findings in IM are merely isolated case reports [4, 5, 11, 12]. Therefore, the present study comprising 28 cases is the largest to date.

Most authors found that on T1W images IM had similar signal intensity to normal muscle tissue [9–13]. However, hyperintense signal of muscle metastases has been also described in the literature [14]. In our series, 91% of IM were isointense in comparison to the unaffected muscle tissue, 4% hypointense and 5% were hyperintense. High signal intensity of metastases on T1W images has been observed in our study in metastases from melanoma, pulmonary angiosarcoma and renal cell carcinoma. In 1 patient with muscle metastasis from pulmonary angiosarcoma areas of haemorrhage within the lesion were found histologically.

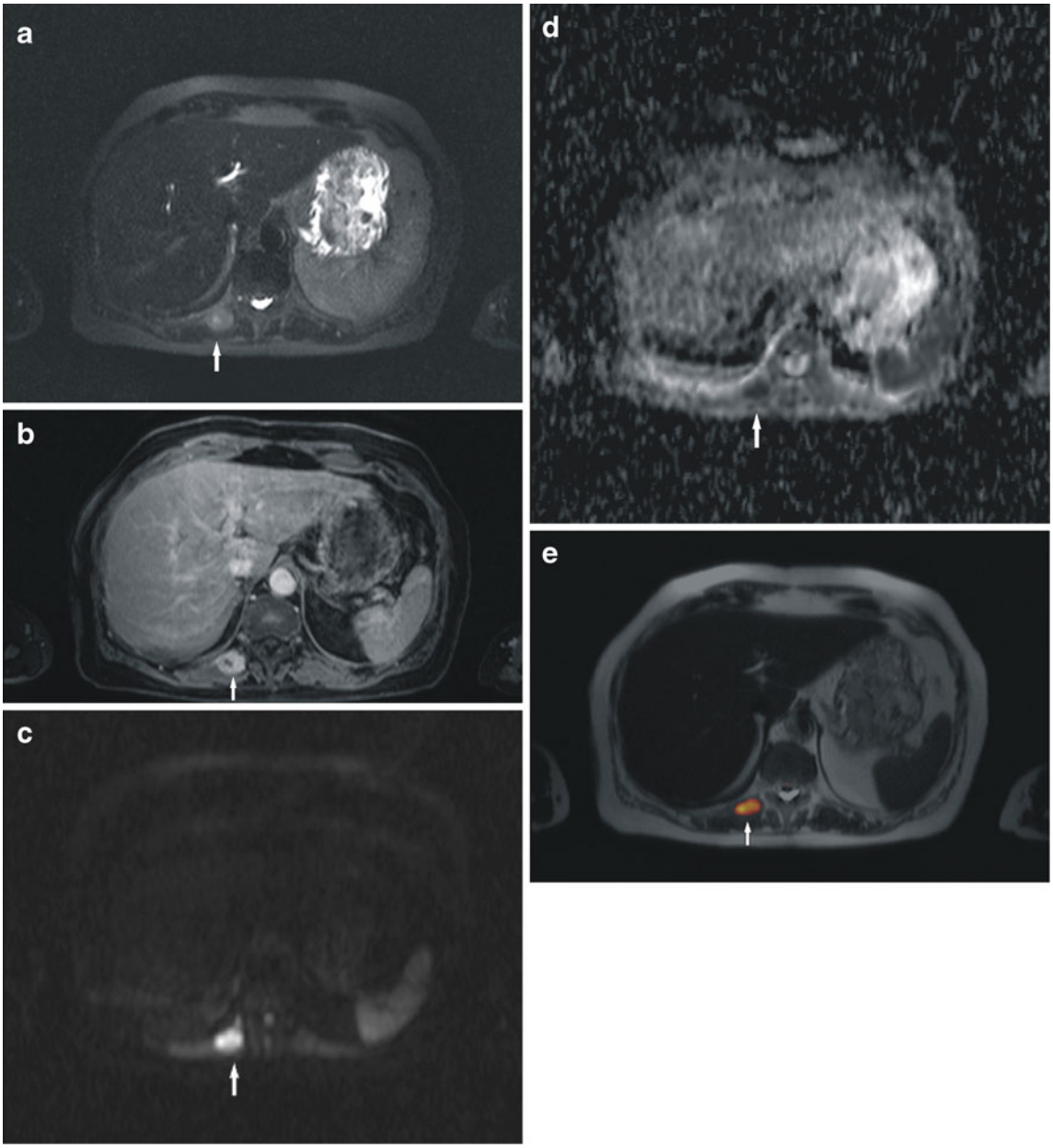

Fig. 3 Imaging findings in a patient with bronchial carcinoma and intramuscular metastasis in the paravertebral musculature (*arrow*). **a** High heterogeneous signal of the metastasis on T2-weighted (T2W) images with fat saturation (HASTE MRI, TR/TE: 800/67). **b** After intravenous administration of contrast medium the lesion (*arrow*) demonstrates a marked signal intensity with central low attenuation (T1 FLASH 2D, TR/TE: 141/2.2). There is no surrounding enhancement.**c** DWI (TR/TE: 3,900/99) of the metastasis with a b-value of 600 s/mm^2. **d** Corresponding ADC map of DWI indicating high cellularity (1.09×10^{-3} mm^{2}s^{-1}). **e** Fusion image between DWI and HASTE images shows a high signal increase within the metastasis (*arrow*)

Table 3 Comparison of apparent diffusion coefficient values in the dependency of signal intensity on fusion images

	Fusion signal intensity			
	0	1	2	3
n	47	23	12	9
ADC values	2.41±0.58	1.77±0.35	1.37±0.16	1.22±0.32

Metastases of malignant melanoma contain melanin, which shows a hyperintense signal on T1W images [14]. On the other hand, melanoma metastases often bleed [14]. However, signal increase on T1W images was seen in only 1 of our 4 patients with melanoma. Signal elevation in metastases of renal cell carcinoma has also been reported [5, 15], but the cause of this constellation is unknown [15]. For this reason some IM can mimic benign muscle lesions, such as lipoma or haemangioma, which are also hyperintense on T1W

images [5, 15, 16]. Another differential diagnosis is intramuscular bleeding. Therefore, other MR investigations of muscle lesions, namely T2W images with fat saturation and application of contrast medium, are needed. However, muscle metastases in renal carcinomas are difficult to differentiate from other malignancies, especially from alveolar soft part sarcomas [5, 16].

On T2W images with or without fat saturation, increased signal intensity is typically seen in muscle metastases [9–13]. Our study showed similar findings.

Some authors suggest that peritumoral edema was seen in most cases [9, 13]. In our series, however, this event was present in only 1.5% of IM on T2W with fat saturation.

According to the literature, other MR techniques, such as DW imaging can provide additional information on soft tissue tumours [17–19]. DWI were described as a useful method of assessment of tumour cellularity in soft tissue sarcomas [18, 20]. Furthermore, these images can be used as a non-invasive tool to monitor treatment responses [21, 22]. In muscle metastases, however, DWI findings have not been described previously.

In our study 91 lesions were analysed on DW images. They showed different ADC values from low to high. Most of the IM (94%) demonstrated moderate or low signal intensity, which suggests relatively high cellularity.

In addition, we performed a fusion between DWI and HASTE images. This approach was successfully used previously in peritoneal carcinosis [23] and has not been reported in cases of muscle metastases. In the present study, 4 patterns of IM could be identified: no abnormal signal (53%), subtle increased signal (28%), moderately increased signal (12%) and highly increased signal (7%). Furthermore, our series shows that the higher the signal on fusion images, the lower the corresponding ADC values. This finding suggests a dependency of fusion signal intensity and tumour cellularity.

According to the literature, after administration of contrast medium, most muscle metastases show marked heterogeneous enhancement associated with tumour necrosis [13]. Thus, extensive peritumoral enhancement has been reported as one of the characteristic features of IM [10]. Therefore, previous reports insisted that MR imaging is not specific enough for IM and that muscle metastases were not easily differentiated from other soft tissue malignancies [9, 10, 12, 13]. In the present study, however, central low attenuation after intravenous administration of contrast medium was seen in 6% of IM. The remaining metastases showed marked homogeneous (88%) or heterogeneous (6%) enhancement. In contrast to other soft tissue malignancies, such as muscle lymphomas or sarcomas [24–26], most of the lesions identified (96%) demonstrated well-defined margins. Therefore, some IM can mimic benign muscle lesions, such as focal myositis [27]. Peritumoral enhancement could be identified in only 2.4%. There was no difference in enhancement characteristics with respect to ADC values or fusion patterns.

In conclusion, MR features of muscle metastases are relatively typical and consist of round or oval intramuscular masses with well-defined margins, marked enhancement, low or moderate ADC values and moderate to high signal intensity on fusion images.

Conflict of interest The authors declare that there is no conflict of interest.

References

1. Kurek J, Nouri S, Kannourakis G, Murphy M, Austin L. Leukemia inhibitory factor and interleukin-6 are produced by diseased and regenerating skeletal muscle. Muscle Nerve. 1996;19:1291–301.
2. Weiss L. Biomechanical destruction of cancer cells in skeletal muscle: a rate-regulator for hematogenous metastasis. Clin Exp Metastasis. 1989;5:483–91.
3. Seely S. Possible reasons for high resistance of muscle to cancer. Med Hypotheses. 1980;6:133–7.
4. Hasegawa S, Sakurai Y, Imazu H, et al. Metastasis to the forearm skeletal muscle from an adenocarcinoma of the colon: report of a case. Surg Today. 2000;30:1118–23.
5. Nabeyama R, Tanaka K, Matsuda S, Iwamoto Y. Multiple intramuscular metastases 15 years after radical nephrectomy in a patient with stage IV renal cell carcinoma. J Orthop Sci. 2001;6:189–92.
6. Willis RA. The spread of tumours in the human body. London: Butterworth; 1952.
7. Glockner DM, White LM, Sundaram M, McDonald DJ. Unsuspected metastases presenting as solitary soft tissue lesions: a fourteen-year review. Skeletal Radiol. 2000;29:270–4.
8. Surov A, Hainz M, Holzhausen HJ, Arnold D, Katzer M, Schmidt J, et al. Skeletal muscle metastases: primary tumours, prevalence, and radiological features. Eur Radiol. 2010;20:649–58.
9. Magee T, Rosenthal H. Skeletal muscle metastases at sites of documented trauma. AJR Am J Roentgenol. 2002;178:985–8.
10. Tuoheti Y, Okada K, Osanai T, et al. Skeletal muscle metastases of carcinomas: a clinicopathological study of 12 cases. Jpn J Clin Oncol. 2004;34:210–4.
11. O'Brien JM, Brennan DD, Taylor DH, et al. Skeletal muscle metastasis from uterine leiomyosarcoma. Skeletal Radiol. 2004;33:655–9.
12. Williams JB, Youngberg RA, Bui-Mansfield LT, Pitcher JD. MR imaging of skeletal muscle metastases. AJR Am J Roentgenol. 1997;168:555–7.
13. Lee BY, Choi JE, Park JM, et al. Various image findings of skeletal muscle metastases with clinical correlation. Skeletal Radiol. 2008;37:923–8.
14. Yoshioka H, Itai Y, Niitsu M, et al. Intramuscular metastasis from malignant melanoma: MR findings. Skeletal Radiol. 1999;28:714–6.
15. Sakamoto A, Yoshida T, Matsuura S, et al. Metastasis to the gluteus maximus muscle from renal cell carcinoma with special emphasis on MR features. World J Surg Oncol. 2007;5:88–92.
16. Nishie A, Stolpen AH, Obuchi M, Kuehn DM, Dagit A, Andresen K. Evaluation of locally recurrent pelvic malignancy: performance of T2- and diffusion-weighted MRI with image fusion. J Magn Reson Imaging. 2008;28:705–13.
17. Bauer A, Reiser MF. Diffusion-weighted imaging of the musculoskeletal system in humans. Skeletal Radiol. 2000;29:555–62.

18. Schnapauff D, Zeile M, Niederhagen MB, et al. Diffusion-weighted echo-planar magnetic resonance imaging for the assessment of tumor cellularity in patients with soft-tissue sarcomas. J Magn Reson Imaging. 2009;29:1355–9.
19. Einarsdóttir H, Karlsson M, Wejde J, Bauer HC. Diffusion-weighted MRI of soft tissue tumours. Eur Radiol. 2004;14(6):959–63.
20. Van Rijswijk CS, Kunz P, Hogendoorn PC, Taminiau AH, Doornbos J, Bloem JL. Diffusion-weighted MRI in the characterization of soft-tissue tumors. J Magn Reson Imaging. 2002;15:302–7.
21. Dudeck O, Zeile M, Pink D, et al. Diffusion-weighted magnetic resonance imaging allows monitoring of anticancer treatment effects in patients with soft-tissue sarcomas. J Magn Reson Imaging. 2008;27:1109–13.
22. Oka K, Yakushiji T, Sato H, Hirai T, Yamashita Y, Mizuta H. The value of diffusion-weighted imaging for monitoring the chemotherapeutic response of osteosarcoma: a comparison between average apparent diffusion coefficient and minimum apparent diffusion coefficient. Skeletal Radiol. 2010;39(2):141–6.
23. Fujii S, Matsusue E, Kanasaki Y, et al. Detection of peritoneal dissemination in gynecological malignancy: evaluation by diffusion-weighted MR imaging. Eur Radiol. 2008;18:18–23.
24. Suresh S, Saifuddin A, O'Donnell P. Lymphoma presenting as a musculoskeletal soft tissue mass: MRI findings in 24 cases. Eur Radiol. 2008;18:1628–34.
25. Eustace S, Winalski CS, McGowen A, Dorfman D. Skeletal muscle lymphoma. Observation at MR imaging. Skeletal Radiol. 1996;25:425–30.
26. Sundaram M. MR imaging of soft tissue tumors: an overview. Semin Musculoskelet Radiol. 1999;3:15–20.
27. Gaeta M, Mazziotti S, Minutoli F, et al. MR imaging findings of focal myositis: a pseudotumour that may mimic muscle neoplasm. Skeletal Radiol. 2009;38:571–8.